

# Variations of the surface ozone content and UV radiation intensity on the Kola Peninsula

V.K. Roldugin, S.A. Rumyantsev, A.Yu. Karpechko, and M.I. Beloglazov

*Polar Geophysical Institute, Kol'skii Scientific Center of the Russian Academy of Sciences, Apatity*

Received March 4, 2004

We present the study of correlation between the intensity of the UV solar radiation and the content of surface ozone in Kola Peninsula for 1999, 2000, and 2001. The diurnal variation has been revealed in the ozone concentration that grows from spring to fall (from ~0% in March to ~20% in September). Statistically significant correlation has been found between the UV radiation and the surface ozone concentration. No influence of the extraterrestrial short-wave UV radiation on the surface ozone has been found. Numerical simulation of the ozone generation and absorption processes in the surface atmospheric layer has shown that the increased diurnal ozone variation in fall may be the result of a combined action of the UV radiation and high concentration of the ozone precursors (the organic peroxyradicals in that case), whose appearance in the atmosphere is characteristic of the summer–fall period.

## Introduction

Ozone forms a significant part of photochemical pollution of the surface atmosphere and absorbs the solar ultraviolet radiation (UVR), being one of the atmospheric greenhouse gases. Tropospheric ozone is the result of photochemical reactions with the participation of nitrogen oxides and the transport from the stratosphere. Both these sources directly or indirectly depend on the intensity of the UV solar radiation. It can affect ozone in two ways: the UV-A radiation results in photodissociation of nitrogen dioxide  $\text{NO}_2$  and ozone generation on the troposphere, while the UV-B radiation leads to photodissociation of ozone with the following formation of OH hydroxyl. It could be expected that the diurnal variation of UVR should manifest itself in the diurnal behavior of the surface ozone concentration (SOC). The diurnal behavior of SOC in the high-latitude regions of the Northern Europe can be found in Refs. 1–4. In Refs. 3 and 4, we discussed qualitatively the relation between the diurnal behavior of SOC and variations of UVR flux on the Kola Peninsula.

Diurnal variations of SOC are determined by the behavior of the most important ozone sources: photochemical generation and transport from the upper troposphere.<sup>5</sup> As was shown experimentally,<sup>5</sup> in summer in the northern Canada the photochemical production is responsible for the major part of the ozone in the atmospheric boundary layer, while the transport from the upper troposphere is the second in significance.

Both the experimental investigations<sup>6</sup> and the results of numerical simulation of photochemical generation of surface ozone<sup>7</sup> indicate that the surface ozone concentration strongly depends on the atmospheric concentration of ozone precursors, that is, substances taking direct part in the ozone production. The most important ozone precursors include organic alkyl peroxyradicals, generated due to oxidation of various components of the biogenic constituents of the air.<sup>7–9</sup> The SOC dependence on the UVR intensity

is determined not only by the direct dependence of the ozone production process, but also by the influence of UVR on the content of the ozone precursors. This can also be influenced by variations of nitrogen oxides during a working day in the regions subject to industrial pollution of air.<sup>10</sup>

Theoretically, the relation between SOC and the UVR intensity depends on many ill-defined parameters. It is interesting to compare directly the SOC variations with the measured UVR intensity in regions with low industrial pollution (and, consequently, with low concentration of nitrogen oxides). This comparison could provide for quantitative determination of the UVR contribution to the generation of surface ozone.

We have studied the relation between UVR and the surface ozone concentration at high-latitude Lovozero station characterized by low industrial pollution.

## 1. Data

For investigation, we used the measurements of the surface ozone content carried out in 1999–2001 at Lovozero station ( $\varphi = 68.0^\circ\text{N}$ ,  $\lambda = 35.1^\circ\text{E}$ ) situated on the Kola Peninsula. The geophysical station in Lovozero, where the measurements were conducted, is located in the forest. Industrial activity near Lovozero is absent. The SOC values measured at Lovozero station correspond to the background high-latitude atmosphere with the minimum industrial pollution. Every minute measurements are being conducted there with a DASIBI-1008 ÅÍ device, whose operating principle is based on measurements of the absorption of UV radiation by the air blown through the device.

Regardless of the obvious physical dependence of the ozone generation and destruction on solar irradiance, the diurnal variations of SOC corresponding to the irradiance variations are clearly pronounced only in the second half of a year. As an example, Fig. 1 depicts the averaged diurnal variations of SOC for the periods of March 11–31 and September 11–30 of 2000 close to the equinox points.

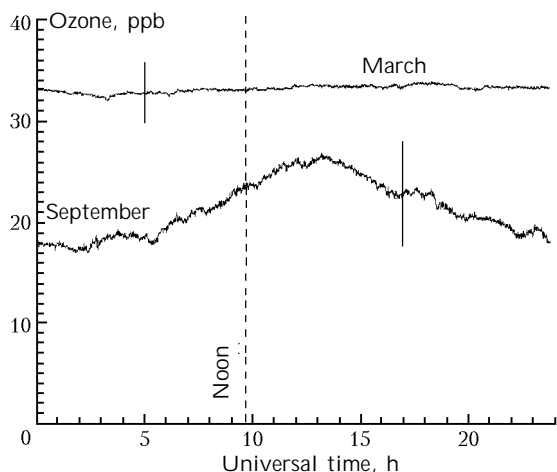


**Fig. 1.** Averaged diurnal variations of the surface ozone concentration.

The vertical bars show typical standard deviations. Local noon occurs at 09:40 UT and is shown by the dashed line. It can be seen that in March the day/night irradiance variations almost do not affect the SOC value. The diurnal variation is less than 1 ppb and much less than the standard deviation. In September, at the similar position of the Sun, the amplitude of the diurnal variation is 20% (about 4.5 ppb) and exceeds the standard deviation. The variation has a peak nearby 13:00 UT, which corresponds to 15:00 LT. At the same time, the surface ozone concentration in September is much lower than in March.

As a diurnal characteristic of SOC, the SOC value averaged over the period from 08:00 to 18:00 UT around the statistically mean diurnal maximum was used. Figure 2a shows the variations of this characteristic for 2000. It can be seen that the ozone content widely varies and changes from 5 to 45 ppb. The bold curve shows the approximation of the annual SOC variation represented by the sum of the first two harmonics with the amplitudes and phases determined by the least-squares method. The maximum and minimum values of the approximated annual SOC variation are ~20 and 35 ppb. The seasonal variation has maximum in April and minimum in November. Similar pattern is observed for other years as well.

The UV radiation intensity in the UV-A (315–400 nm) and UV-B (280–315 nm) regions is being measured at the Polar Geophysical Institute with a network GGO M-124 device installed on an atmospheric station in Apatity ( $\phi = 67.6^\circ\text{N}$ ,  $\lambda = 33.4^\circ\text{E}$ ) located at a distance about 90 km from Lovozero. The M-124 device measures the net radiation incident on a horizontal surface. Its relative error does not exceed 15%. Calibration and verification of the M-124 device are carried out at GGO (Main Geophysical Observatory) once every two years. The measurements are conducted roughly once an hour at the sun elevation angles larger than  $10^\circ$  under conditions with no precipitation. In August–September 2001 the UVR observations were not conducted because the M-124 device was at the calibration site.

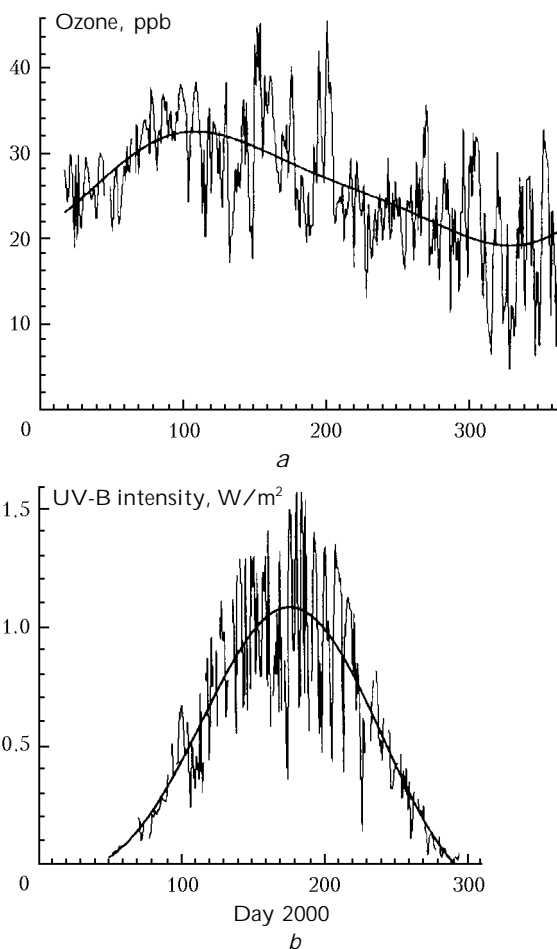


**Fig. 2.** Average diurnal values of the surface ozone concentration at Lovozero station (a) and UV radiation in Apatity (b) in 2000. Bold line shows the approximation by the first two harmonics.

In Apatity, the surface ozone content is also measured with a chemiluminescent ozonometer, whose calibration is a little bit complicated. The experiment demonstrates similar SOC variations at stations Apatity and Lovozero, and the similarity is inherent not only in diurnal or seasonal variations, but also in the variations caused by changes in weather. In this paper we use the SOC measurements obtained in Lovozero, rather than those obtained in Apatity because of the well-defined absolute values of the former.

The radiation in both UV-A and UV-B regions exhibits the diurnal behavior affected by the weather conditions. As an example, Fig. 3 shows the measurements in UV-A nearby the equinox points in 2000 as a function of time of a day. The curves show the approximations by cubic parabolas representing the mean diurnal variation for the periods nearby the equinoxes. The UV-A intensity in March is higher than in September. This can be caused by both the higher atmospheric transparency and lower cloudiness and by the enhanced (due to the snow cover) albedo in March. As known,<sup>11</sup> the intensity of solar UVR in polar regions in spring can significantly exceed that during the fall.

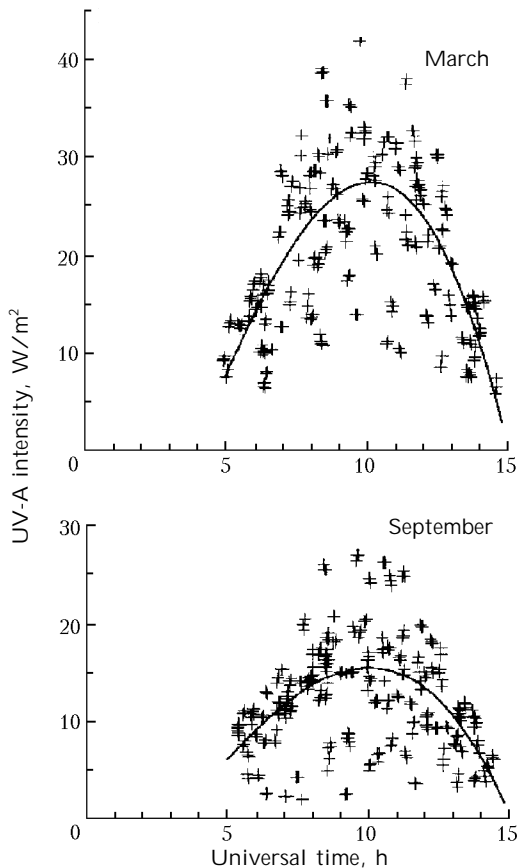


Fig. 3. Measurement data on UV-A in March 11–31 and September 11–30 of 2000 as functions of the universal time.

As diurnal UVR characteristics, we took the values of the UV-A and UV-B intensity in the period from 08:00 to 12:00 UT, that is, near the local solar noon. Figure 2*b* shows the UV-B intensity for 2000 determined in this way. We can see a wide day-to-day variability of the average characteristic of the UV-B intensity, whose fluctuations can achieve a half of the mean level. Weather factors play the decisive role in this variability. The bold curve shows the approximation by the first two harmonics.

## 2. Correlation analysis

It seems interesting to find whether or not there is a statistical correlation between the SOC and UVR variations on the time scale of several days. Correlation analysis of the initial data makes no real sense, because both of the characteristics undergo strong seasonal variations, and just these variations will determine the magnitude of the correlation coefficient. The annual variations of SOC and UVR were approximated by the sum of two first harmonics (see Fig. 2). The seasonal components processed in this way have thus been excluded, and the comparison was performed for the differences between the total values and the seasonal variations.

In Fig. 4, the solid curves show the autocorrelation functions of the SOC differences (thin line) and UV-

A intensity (thick line) for 2000. For two other years as well as for UV-B the dependences are similar. It can be seen that already at a 1 or 2-day shift, the functions drop down to insignificant values, that is, the values of both characteristics on some day are independent of their values on previous days. For such processes the correlation coefficient can bear certain meaning.

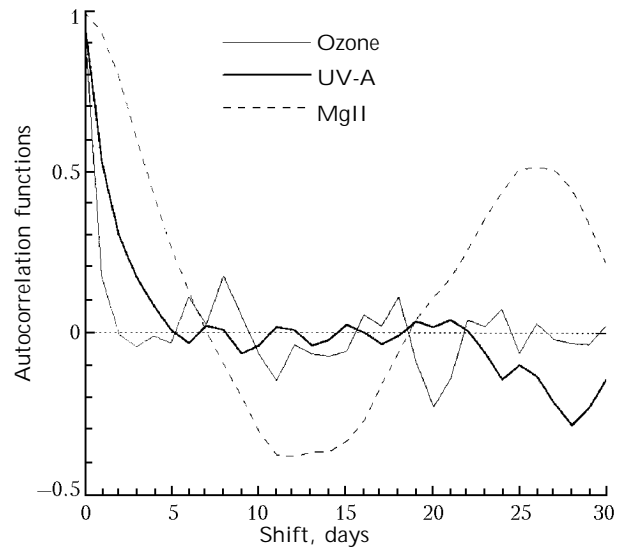


Fig. 4. Autocorrelation functions of SOC and UVR (UV-A) variations without annual components for 2000, along with the MgII index for the same year.

The coefficients of correlation  $r$  between variations of SOC and UV-A or UV-B for three years are summarized in the Table. The Table also presents the confidence intervals  $\Delta r$ , calculated by the equation from Ref. 12 at 95% probability level:

$$\Delta r = 1.96 \frac{1 - r^2}{\sqrt{N - 1}}, \quad (1)$$

and the number of data pairs  $N$ , that is, days, from which the correlation was calculated. Significant, according to this equation, correlation coefficients are printed in bold. The calculations were performed using data both for the whole year and for August–September (in 2001 for June–early July), the period of the maximum in the diurnal variation.

The most (10 of 12) correlation coefficients proved to be significant, and the correlation is positive, though the coefficients are not high. It can also be seen that for the summer months, when the diurnal variation is pronounced, the correlation is higher than for the whole year.

Strictly speaking, Eq. (1) not fully determines the significance of the correlation coefficients, because it assumes the Gaussian distribution of residues, which is not always true in practice. More serious arguments in favor of the correlation between SOC and UVR intensity variations are their cross-correlation functions. They have rather narrow main peaks near the zero shift, and, as a rule, additional peaks at a one-day lag of SOC relative to the UVR peak.

Correlation coefficients of diurnally mean values of surface ozone at station Lovozero with various optical parameters

Period	UV-A		UV-B		MgII	
	$r \pm \Delta r$	$N$	$r \pm \Delta r$	$N$	$r \pm \Delta r$	$N$
1999, all data	$0.098 \pm 0.148$	174	<b><math>0.199 \pm 0.143</math></b>	174	$-0.023 \pm 0.128$	237
August–September 1999	<b><math>0.260 \pm 0.251</math></b>	54	<b><math>0.294 \pm 0.246</math></b>	54	$0.140 \pm 0.280$	48
2000, all data	<b><math>0.147 \pm 0.131</math></b>	215	<b><math>0.152 \pm 0.131</math></b>	215	<b><math>0.173 \pm 0.122</math></b>	243
August–September 2000	<b><math>0.272 \pm 0.238</math></b>	59	$0.153 \pm 0.263$	54	$-0.041 \pm 0.282$	49
2001, all data	<b><math>0.302 \pm 0.144</math></b>	155	<b><math>0.313 \pm 0.142</math></b>	155	$0.041 \pm 0.125$	248
June–July 2001	<b><math>0.434 \pm 0.258</math></b>	39	<b><math>0.397 \pm 0.268</math></b>	39	$0.024 \pm 0.267$	55

Figure 5 shows the cross-correlation functions of SOC and UV-A calculated for all data for each of the three years. As in the above, the deviations from the seasonal approximations for SOC and UV-A were taken.

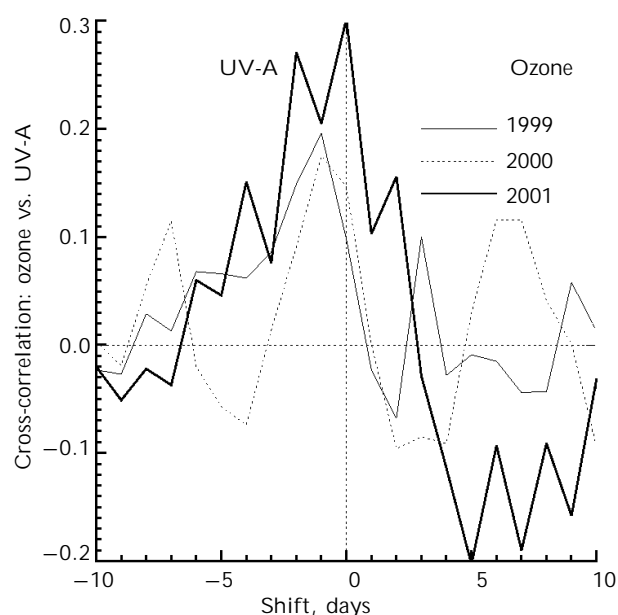


Fig. 5. Cross-correlation functions of SOC and UV-A intensity for 1999–2001 for all data.

In Fig. 5, the physical characteristics that become advanced in the case if the curve maximum is located on their side are shown on both sides from the zero lags. Since the tabulated correlation coefficients are given for zero shifts, they are understated, if the maximum is shifted by one day toward the UVR advance. Thus, for all pairs of 1999 (see Fig. 5) the insignificant coefficient  $0.098 \pm 0.148$  becomes significant  $0.196 \pm 0.144$ , and for 2000 the value of 0.147 should be replaced by 0.175.

The same functions have been calculated for UV-B and summer periods as well; in general, they turned out to be similar to the dependences shown in Fig. 5. Therefore, it can be concluded that there is a positive correlation between the SOC and UVR variations in the period of several days with the SOC variations lagging roughly by one day. No significant difference was found between the correlations of SOC with UV-A and UV-B radiation; both these correlations have the positive sign and close values. If we interpret this result in terms of photochemical reactions, then it means the prevalence of the effect of  $\text{NO}_2$  dissociation over the ozone dissociation.

### 3. Surface ozone and extraterrestrial UVR

The correlation between the UVR intensity and SOC is not finally established. Thus, in Ref. 13 the comparison of the average annual values of the UV-B intensity and SOC for two solar cycles has shown that the SOC variation with the three-year shift copies well enough the variation of the UV-B flux. It has been concluded that the UVR does not directly determine the ozone generation in the troposphere.

The deviations of UVR from the average seasonal values considered in this paper are determined by two factors: (1) the conditions of UVR penetration through the atmosphere and (2) variations of extraterrestrial UV radiation due to the varying solar activity. The latter is more significant for UV-B. Therefore, it seems interesting to compare SOC with the intensity of extraterrestrial UVR independent of the atmospheric conditions.

As a parameter determining the intensity of the solar radiation in the UV region, we took the diurnal values of the MgII index. This index, determined from the data of the SBUV satellite borne UV spectrometer since November 1987, is calculated from the width of the Mg 278 nm doublet and characterizes the variations of solar radiation in the region of 175–290 nm [Ref. 14].

The comparison of the average diurnal variations of SOC and the MgII index allows us to judge on the direct correlation between surface ozone and the short-wave solar UV radiation. The Table gives the values of the correlation coefficient for SOC and the MgII index. Formally, this coefficient turned out to be significant only in one of six considered cases, namely, for all values of 2000. Indeed, the visual comparison of the variations of both of the parameters in summer of 2000 reveals some similarity. However, this similarity is only accidental: neither for 1999 nor for 2001 the correlation was observed between these parameters for summer and for the whole year. In addition, the alarming circumstance is that the correlation coefficient is negative for two of six cases in the Table. The cross-correlation functions have demonstrated the physical inconsistency of formal significance: the peaks proved to be wide and advanced with respect to both the MgII index and SOC.

The autocorrelation function of the MgII index shown by the dashed curve in Fig. 4 differs from the corresponding functions for SOC and UVR not only

by the width of the main peak, but also by the pronounced 27-day peak caused by the rotation of the sun. In two other curves, the 27-day maximum is absent, which is also indicative of the absence of significant correlation of the SOC and UVR variations with the variations of extraterrestrial short-wave UVR. These data demonstrate that either there is no 27-day periodicity in the SOC variations or its contribution is insignificant.

Thus, no direct effect of the extraterrestrial UVR variations on the concentration of the surface ozone near Lovozero was found.

#### 4. Simulation

The observations show that, at Lovozero station under close-to-background conditions of anthropogenic pollution, the effect of UVR on surface ozone increases from spring to fall and is most pronounced in the diurnal variations of SOC in August–September. The correlation between the UVR intensity and SOC increases from March, when the diurnal variation is small, to September, when the amplitude of the diurnal variation achieves 20%. This behavior may be caused both by the atmospheric chemical processes and the dynamics of atmospheric air. Consider the role of the first group of processes. Though the transport also contributes to the distribution of surface ozone,<sup>1</sup> we restrict our consideration to the effect of photochemical processes. The role of convective exchange in the atmosphere and the temperature will be the subject of the next paper.

For numerical calculation, we used a simple one-box model adequately describing the processes in the mixing layer, which is considered in detail in Ref. 15. This model adequately describes the main characteristics of distribution of ozone and other trace gases under the background and polluted conditions.<sup>16,17</sup> In an ideal case, the concentration of trace gases in the mixing layer is assumed homogeneous.<sup>18</sup> This assumption is confirmed for volatile organic compounds (VOCs), for which a relatively homogeneous distribution in the mixing layer was found experimentally.<sup>19</sup> In the model used, the distribution of all trace gases in the mixing layer is taken constant with height.

The model describes the chemical transformation of nine independent gases: O<sub>3</sub>, NO, NO<sub>2</sub>, NO<sub>3</sub>, N<sub>2</sub>O<sub>5</sub>, HNO<sub>3</sub>, CH<sub>3</sub>O<sub>2</sub>, PAN (peroxyacetyl nitrate), and HO<sub>2</sub>. They react with each other and with UVR in 30 reactions, representing the main interactions, occurring in the surface atmosphere and including three reactions of photodissociation of NO<sub>2</sub> and NO<sub>3</sub>. The list of the reactions used can be found in Ref. 15, the reaction rates are borrowed from Refs. 20 and 21, the rate of reaction of NO with organic alkyl peroxyradicals RO<sub>2</sub> is taken from Ref. 22. It is assumed that atomic oxygen produced immediately transforms into ozone. The following compounds were considered as the preset ones: molecular hydrogen, water vapor, hydroxyl, carbon monoxide, formaldehyde, methane, and organic alkyl peroxyradicals RO<sub>2</sub>.

In the model, the equations of chemical kinetics with allowance for dry sedimentation were solved

$$dn_i/dt = S_i - L_i - (v_i n_i/h), \quad (2)$$

where  $n_i$  is the concentration of the  $i$ th component,  $i = 1, 2, 3, \dots, 9$ ;  $S_i$ ,  $L_i$  are the terms describing the sources and losses of the  $i$ th component;  $v_i$  is the dry sedimentation rate;  $h$  is the height of the mixing layer. The source  $S(\bar{I}_3)$  for ozone includes the term  $S_n(\bar{I}_3)$ , describing the ozone generation in chemical reactions, and the term  $S_t(\bar{I}_3)$ , corresponding to the ozone inflow from the free troposphere:  $S(\bar{I}_3) = S_n(\bar{I}_3) + S_t(\bar{I}_3)$ . Similarly, the source  $S(\text{NO})$  for nitrogen monoxide includes the term  $S_c(\text{NO})$ , caused by chemical transformations, and the term  $S_t(\text{NO})$ , representing the NO inflow from the lower boundary of the mixing layer. The sources  $S_i$  for the other components are assumed zero for simplicity.

The photodissociation rates of NO<sub>2</sub> and NO<sub>3</sub> and the concentrations of OH hydroxyl and important ozone precursors – organic alkyl peroxyradicals RO<sub>2</sub> were specified as functions of local time, namely, the positive branch of the sine function in the period of solar irradiation of the atmosphere with a peak at full sun and zero at the sun below the horizon. In the light period, the main mass of volatile organic compounds is injected and hydroxyl is generated, which results in formation of RO<sub>2</sub> in the reactions of hydroxyl with VOCs.<sup>7–9</sup> The maximum hydroxyl concentrations were determined through parameterization described in Ref. 23. The dry sedimentation rates were taken from the literature independent of time of a day. For ozone, we used the results of Ref. 24 for Alaska with the values  $v(\text{O}_3) = 0.007$  m/s for the summer and fall,  $v(\text{O}_3) = 0.0005$  m/s for winter; and for the spring we used  $v(\text{O}_3) = 0.004$  m/s from Ref. 25. For other gases, the following values were taken:  $v(\text{NO}_2) = 0.003$  m/s [Ref. 26],  $v(\text{NO}_3) = v(\text{N}_2\text{O}_5) = v(\text{HNO}_3) = v(\text{CH}_3\text{O}_2) = 0.02$  m/s [Ref. 27],  $v(\text{PAN}) = 0.0026$  m/s [Ref. 28]. The dry sedimentation rate of NO was assumed zero.

The UVR intensity enters into Eqs. (2) through the photodissociation rates. The behavior of the model at different levels of UVR was studied in Ref. 17. For the photodissociation rate of nitrogen dioxide in different seasons, we used the value  $\sim 5 \cdot 10^{-3} \cdot \text{s}^{-1}$  obtained on Spitsbergen.<sup>11</sup> The value of  $S_t(\text{O}_3)$  was taken such that the ozone concentrations in the model calculations at 00.00 and 24.00 to be the same and equal to  $\sim 10^{-5}$ – $10^{-4}$  ppb.

The equations of chemical kinetics (2) were solved by the variable-order Gear's method with a variable step for rigid systems. The calculated SOC variations during a day in the equinox periods are depicted in Fig. 6.

The initial content of nitrogen oxides NO<sub>x</sub> = NO + NO<sub>2</sub> and the intensity of the NO source were set such that the NO<sub>x</sub> concentration to be within 1 ppb. This value roughly corresponds to the boundary between nonpolluted and polluted conditions. The maximum photodissociation rate of NO<sub>2</sub> is  $6 \cdot 10^{-3} \text{ s}^{-1}$  at the spring equinox and  $3 \cdot 10^{-3} \text{ s}^{-1}$  at the fall

equinox, and the UVR intensities in these periods also differ roughly twice (see Fig. 3). The average diurnal air temperature was taken equal to  $-10^{\circ}\text{N}$  at the spring equinox and  $+10^{\circ}\text{N}$  at the fall equinox. The concentrations of such ozone precursors as methane, carbon monoxide, and hydroperoxyl  $\text{HO}_2$  are weakly connected with biological changes in the nature, and the corresponding SOC variations are small, as has been shown by the calculations.

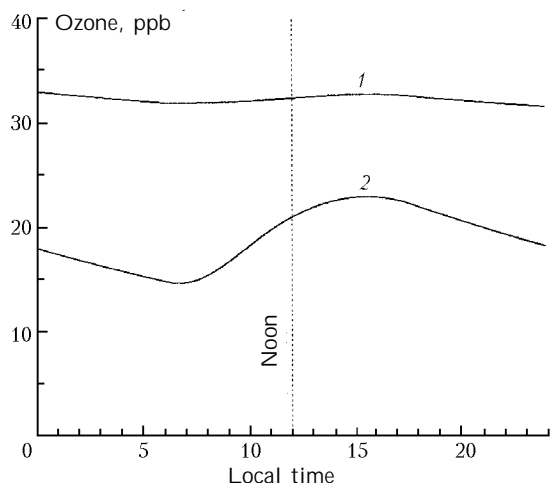


Fig. 6. Model diurnal SOC variation in the periods of spring (curve 1) and fall (curve 2) equinox.

At the same time, an important difference between the spring and fall equinox is the low spring concentration (or absence) of such ozone precursors as organic alkyl peroxyradicals  $\text{RO}_2$ , which are largely of biogenic origin.<sup>7</sup> In the example under consideration, the following values were used:  $[\text{RO}_2] = 0$  in the spring (when the ground is covered by snow in the high latitudes) and  $[\text{RO}_2] = 30$  ppt in the summer and the fall (in the presence of the plant cover). This value is taken from the model results on  $\text{RO}_2$  production by plants upon oxidation of organic biogenic components of air.<sup>9</sup> The higher value of the mean SOC in the spring (curve 1 in Fig. 6) is caused by larger ozone inflow from above in the spring ( $S_t \sim 10^{-4}$  ppb/s) than in the fall, and it reflects the role of the source of surface ozone connected with the transport from the stratosphere.

It can be seen from Fig. 6 that the diurnal variations of SOC in the spring is low. It is caused by the interaction of  $\text{HO}_2$  with  $\text{NO}_x$  at the existing level of UVR. The significant diurnal variation of UVR at the low content of  $\text{NO}_x$  (catalysts of transformation of the ozone precursors into ozone), which is characteristics of weakly polluted regions, in this period does not lead to marked variations of SOC. In the fall, as can be seen from curve 2 in Fig. 6, the diurnal variation is well pronounced, achieving tens per cent (amplitude  $\approx 20\%$ ), and caused by the fact that in the model we used quite high, as compared to the spring level,  $\text{RO}_2$  content at the constant  $\text{NO}_x$  content. The SOC peak is achieved at  $\sim 15.00$  local solar time, which corresponds to 13.00 UT for Lovozero station.

Thus, according to the model calculations, the spring concentration of the ozone precursors  $\text{RO}_2$  is too low to cause the significant SOC variation during a day. In the fall, the content of the ozone precursors  $\text{RO}_2$  is much higher and causes large diurnal variation of the ozone, in spite of the decrease in the UVR intensity as compared to the spring. The comparison of the model results (see Fig. 6) with the experimental data depicted in Fig. 1 shows that the diurnal variation of SOC can be explained by the interaction of the ozone precursors and UVR with participation of the catalysts  $\text{NO}_x$ . Another factor causing the diurnal SOC variation is the diurnal variation of the surface temperature, which was neglected in this work.

## Conclusions

The experimental study of the correlation between the solar UV radiation and the surface ozone concentration at Lovozero station (Kola Peninsula) in 1999–2001 has revealed significant UVR/SOC correlation; the annual and diurnal variations of the ozone concentration and the UVR intensity have been drawn, and the numerical approximations for the annual dependences have been constructed. The numerical simulation of the ozone generation and destruction in the surface layer confirms the hypothesis that the increased diurnal variation of SOC at the fall equinox can be caused by the joint effect of UVR and high concentrations of the ozone precursors, namely, organic alkyl peroxyradicals, whose presence in the surface air is characteristic of the summer–fall period. The ozone generation in the surface layer near Lovozero station is determined not only by the UV radiation influx, but also by the presence of the ozone precursors in the surface air.

## Acknowledgments

This work was supported, in part, by the Russian Foundation for Basic Research (grants No. 02-05-64114 and No. 02-05-79148), INTAS-01-0016, INCO-COPERNICUS (grant No. ICA-2000-10038), and the Program of Basic Research of the Physical Sciences Division of RAS.

## References

1. T. Laurila and H. Lattila, *Atmos. Environ.* **28**, No. 1, 103–114 (1994).
2. T. Laurila, *Geophysics* **32**, Nos. 1–2, 167–193 (1996).
3. V.F. Larin, M.I. Beloglazov, A.N. Vasil'ev, and S.A. Rumyantsev, *Geomagnetizm i Aeron.* **36**, No. 2, 173–174 (1996).
4. V.F. Larin, M.I. Beloglazov, A.N. Vasil'ev, and S.A. Rumiantssev, *Ann. Geophys.* **15**, No. 12, 1615–1616 (1997).
5. D.L. Mauzerall, D.J. Jacob, S.-M. Fan, J.D. Bradshaw, G.L. Gregory, G.W. Sachse, and D.R. Blake, *J. Geophys. Res. D* **101**, No. 2, 4175–4188 (1996).
6. B.D. Belan and T.K. Sklyadneva, *Meteorol. Gidrol.*, No. 5, 50–60 (2001).
7. V.A. Isidorov, *Organic Chemistry of the Atmosphere* (Khimizdat, St. Petersburg, 2001), 352 pp.

8. S.M. Semenov, in: *Investigations in the Field of Oceanology, Atmospheric Physics, Geography, Ecology, Water Problems, and Geocryology* (GEOS, Moscow, 2001), pp. 173–179.
9. P.A. Makar, J.D. Fuentes, D. Wang, R.M. Staebler, and H.A. Wiebe, *J. Geophys. Res. D* **104**, No. 3, 3581–3603 (1999).
10. M.I. Beloglazov, A.Yu. Karpechko, G.N. Nikulin, and S.A. Rumyantsev, *Meteorol. Gidrol.*, No. 3, 57–63 (2001).
11. H. Beine, A. Dahlback, J.B. Ørbæk, *J. Geophys. Res. D* **104**, No. 13, 16009–16019 (1999).
12. I.N. Bronshtein and K.A. Semendyaev, *Mathematics Handbook* (Nauka, Moscow, 1986), 464 pp.
13. M.Yu. Arshinov, B.D. Belan, V.E. Zuev, O.A. Krasnov, V.A. Pirogov, T.K. Sklyadneva, and G.N. Tolmachev, *Atmos. Oceanic Opt.* **15**, No. 11, 896–901 (2002).
14. M.D. DeLand and R.P. Cebula, *J. Geophys. Res. D* **98**, No. 7, 12809–12823 (1993).
15. S.A. Rumyantsev and V.K. Roldugin, *Ekol. Khimiya* **12**, No. 2, 69–78 (2003).
16. S.A. Rourmiantsev and V.C. Roldugin, in: *Proc. of the XXIII Annual Seminar on Physics of Auroral Phenomena* (Apatity, 2001), pp. 115–117.
17. V.K. Roldugin, S.A. Rumyantsev, A.Yu. Karpechko, and M.I. Beloglazov, in: *Kola Peninsula on the Verge of the Third Millennium. Environmental Problems*, ed. by N.A. Kashulin (Apatity, 2003), pp. 50–58.
18. B.D. Belan, *Atmos. Oceanic Opt.* **7**, No. 8, 558–562 (1994).
19. J.P. Greenberg, A. Guenter, P. Zimmerman, W. Baugh, C. Geron, K. Davis, D. Helmig, and L.F. Klingler, *Atmos. Environ.* **33**, No. 6, 855–867 (1999).
20. J. Crawford, D. Davies, J. Olson, G. Chen, S. Liu, G. Gregory, J. Barrick, G. Sachse, S. Sandholm, and B. Heikes, *J. Geophys. Res. D* **104**, No. 13, 16255–16273 (1999).
21. R.A. Zavery and L.K. Peters, *J. Geophys. Res. D* **104**, No. 23, 30387–30415 (1999).
22. T. Staffelbach, A. Neftel, A. Blatter, A. Gut, M. Fahrni, J. Staähelin, A. Prévôt, A. Hering, M. Lehning, and B. Neininger, *J. Geophys. Res. D* **102**, No. 19, 23345–23362 (1997).
23. L. Ganzveld and J. Lellieveld, *J. Geophys. Res. D* **100**, No. 10, 20999–21012 (1995).
24. A.H. Goldstein, S.C. Wofsy, and C.M. Spivacovsky, *J. Geophys. Res. D* **100**, No. 12, 21023–21033 (1995).
25. T.A. Markova, "Spatial and Temporal Variation of Ozone Concentration in the Surface Atmospheric Layer," Author's Abstract of Phys. Math. Sci. Cand. Dissert., Moscow State University, Moscow (2002).
26. F.Ya. Rovinskii and V.I. Egorov, *Ozone, Nitrogen and Sulfur Oxides in the Lower Atmosphere* (Gidrometeoizdat, Leningrad, 1986), 183 pp.
27. P. Sander and P.J. Crutzen, *J. Geophys. Res. D* **101**, No. 4, 9121–9138 (1996).
28. S. Wunderly and R. Gerig, *Atmos. Environ.* **25A**, No. 8, 1599–1608 (1991).